

A New Spectroheliograph System on the Domeless Solar Telescope at Hida Observatory

Satoru UeNo, Kiyoshi Ichimoto, Yoshikazu Nakatani, Reizaburo Kitai,

Kazunari Shibata, Shin'ichi Nagata, Goichi Kimura

(2010. 4. 22)

Hida Observatory, Kyoto University,

Kurabashira, Kamitakara, Takayama, Gifu 506-1314

ueno@kwasan.kyoto-u.ac.jp

KeyWords: Spectroheliograph --- Spectroscopy --- Sun: Chromosphere

Abstract

In order to obtain spectral information with high spatial and spectral resolutions and with a high time cadence, a new spectroheliograph system was equipped on the Domeless Solar Telescope (DST) at Hida observatory. High sensitivity and high frame rate CCD cameras were installed together with an image scanning mechanism for this purpose. With the new system, we can obtain a spectroheliogram for a middle-size active region in 10 - 20 sec at Ca II H or K lines. Observing wavelength is flexibly chosen from violet to near infrared range, and simultaneous observation in multiple wavelengths is also possible. The new spectroheliograph system provides a powerful tool for the diagnosis of the ubiquitous dynamic phenomena recently found in chromospheres by the Solar Optical Telescope aboard Hinode. So far, we have been observing various target regions on the sun mainly in CaII H/K and $H\alpha$ in coordination with the Hinode. This paper describes the basic features of the new observing system at DST.

1. Introduction

Since the Hinode satellite was launched and started solar observations in 2006, the Solar Optical Telescope (SOT) revealed the remarkably dynamic nature of the chromosphere with its Ca II H filtergraph; tiny jets, possibly driven by magnetic reconnections, are regularly generated everywhere

in the chromosphere (ubiquitous reconnection, Shibata et al. 2007), especially short-lived faint jets are discovered in sunspot penumbra (Katsukawa et al. 2007). The spicules, which are more general chromospheric jets, show lateral oscillatory motions (De Pontieu et al. 2007) and fibered structures of prominences also show clear evidence of oscillations (Okamoto et al. 2007, Ning et al. 2009); these observations suggest the persistent presence of Alfvén or kink-mode waves in the corona. SOT also found small scale magnetic fields covering entire solar photosphere; in Stokes-V, tiny flux tubes are found to be shuffled by the convective motions of granule, and in Stokes-Q,U, ubiquitous horizontal magnetic fields are found to appear and disappear in a short time scale (Lites et al. 2007, Ishikawa et al. 2008). Dynamical responses of the upper atmosphere to such photospheric activities would be the key for understanding the coronal / chromospheric heating. Detailed diagnostics, i.e., quantitative measurements of physical quantities, of the small scale dynamics in chromospheres are of a crucial importance for understanding the basic process taking place in these phenomena, and for further exploration of the origin of the solar atmosphere.

Only with the broad-band filtergraph of the SOT in Ca II H, however, it is not possible to obtain physical quantities such as temperature, velocity and density, nor information about the variation along the line of sight. Spectroscopic observations, which enable us to investigate three dimensional structures of physical quantities, are thus important and highly complementary to the SOT observation.

Typical time-scale of the chromospheric dynamic phenomena is a few ten seconds or a few minutes. To know the time-evolution of these chromospheric phenomena, we have to obtain a set of spectral data within a period enough shorter than their evolutionary time-scale. However the typical duration for scanning over an active region with traditional spectroheliographs are about a minute or longer in Ca II H/K absorption lines, and it is not compatible with the study of the dynamic chromospheric phenomena. To meet the observational requirement, we equipped high sensitivity and high

frame-rate CCD cameras on the spectroscopes of the Domeless Solar Telescope (DST) at Hida Observatory in 2007.

In this paper, we describe the basic features of our new spectroheliograph system, with some examples of data obtained with the system.

2. Domeless Solar Telescope and its Spectrograph

The Domeless Solar Telescope (DST) at Hida Observatory is a 60cm aperture Gregorian telescope dedicated for high spatial resolution observations of the sun (Nakai,Y. and Hattori,A. 1985). The telescope is mounted on the top of a tower at a height of 22m from the ground. Temperature of side walls of the tower is kept as a few degree C lower than the ambient temperature to minimize the air turbulence caused by sunshine on the wall. Entire optical path from the entrance window of the telescope to the observing room is evacuated to mitigate the air turbulence in the telescope. The telescope has an effective focal length of 32.19 (F53.7) and creates solar image (6.41arcsec/mm) on the focal plane in observing rooms at the ground level.

DST has two spectrographs: "Vertical Spectrograph (VS)" and "Horizontal Spectrograph (HS)" (figure 1). The VS gives a high spectral dispersion with a large grating to achieves a wavelength-resolution ($\lambda/d\lambda$) of 1290000 in the 5-th order spectrum around 630 nm. We use the VS for high-resolution and high-dispersion spectroscopy, but with a small coverage of wavelength at one time. On the other hand, the HS is used for multi-wavelength spectroscopy in which we can simultaneously observe different wavelengths covering from UV to near infrared. The HS has three gratings and one of them is selectable to optimize the observation parameters. One of the VS and HS is selected according to the observational purposes by inserting or removing a folding-mirror at the exit window of the telescope (see figure 1). The basic parameters of the two spectrographs are

summarized in Table-1.

By using these spectroscopes, we have been performing spectroheliographic observations using slow CCD cameras with a mechanical shutter (low time cadence) or video cameras (small format and less photometric accuracy, Hanaoka 2003). The quantum efficiency and pixel size of these CCD cameras were typically around 28 % at or less CaII H and K wavelength and 9 micron/pixel. Solar image was scanned in perpendicular to the slit by maneuvering the telescope, which also limit the cadence of scanning observations.

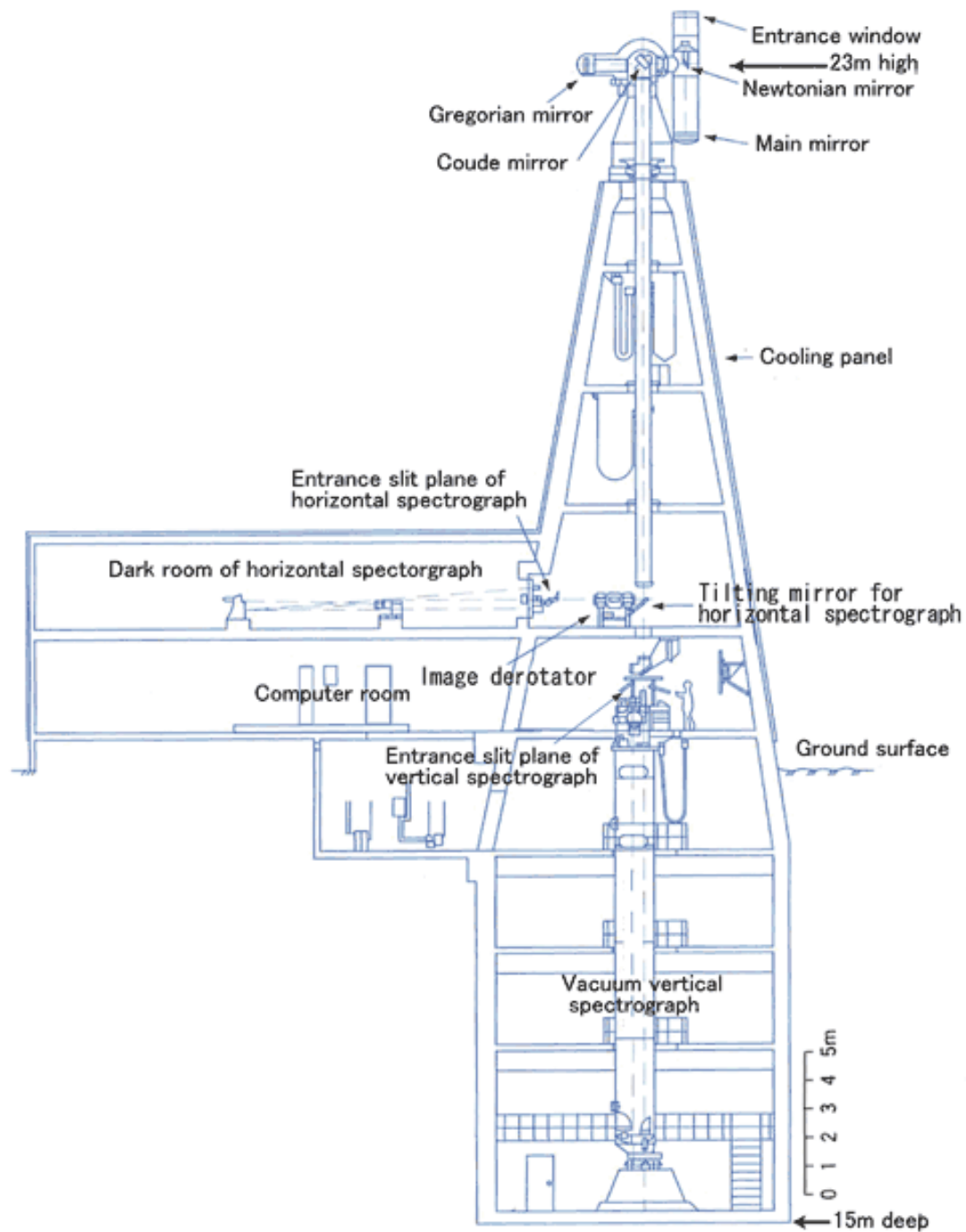


Fig. 1 The cross section of the Domeless Solar Telescope (DST) and positions of Vertical Spectrograph (VS) and Horizontal Spectrograph (HS).

Table 1 Basic parameters of the spectrograph of DST

	HS	VS
Configuration	Zerney-Turnar	Zerney-Turnar vacuum
Focal length	10m	14m
Grating	selectable 3 gratings	
Size	20.6 cm x15.4 cm	40.8 cm x 30.6 cm
Groove density	600 or 1200/mm	632/mm
Blaze angle	13, 17, 23 degree	56 degree
Dispersion (typical)	0.33 Å/mm (2nd order)	0.14 Å/mm (5th order)
Effective wavelength range	3600 - 16000 Å	3600 - 16000 Å
Note	Simultaneous observation of all the visible spectrum	High dispersion with high resolution

3. Feature of the new spectroheliograph system

To meet with the recent requirements from observations to study the fine scale dynamic phenomena in chromosphere, the spectroheliograph system of the DST was improved by installing new CCD cameras and an image scanning mechanism. The new CCD cameras are Prosilica 1650E whose basic specification are summarized in Table 2.

Table 2 Specification of the CCD camera

Product ID	Prosilica 1650E
Device type	Interline CCD
Format	1600 x 1200 pixels
Pixel size	7.4 μm x 7.4 μm
Wavelength range	3100 ~ 11000 \AA (QE ~47% around 3900 \AA)
Exposure time	10 μs – 60 sec (typical in observation; 0.050 – 0.100 s around 3900 \AA)
Full well	20,000 e^-
AD conversion	12bit
Read noise	20 e^-
Interface to PC	Giga eathernet
Frame rate	30 frames/sec (max)
Operation software	Windows XP

The cameras are attached on the exit ports of the spectrographs with a relay lens system that reduces the spectral image with a factor of 0.39. Thus the pixel scale gets 0.12 arcsec/pix (0.24 arcsec/pix in 2x2 binning) in spatial direction with the spatial coverage (FOV along the slit) of 145 arcsec. Wavelength dispersion of VS and HS are shown in figure 2 as a function of wavelength. We consider the appropriate dispersion for the spectrum measurement of Ca II K or H line is around 0.02 $\text{\AA}/\text{pix}$. Therefore, we select 2nd order spectra for both spectrographs, when we observe those lines. More concretely, pixel scales in wavelength are 0.010 $\text{\AA}/\text{pix}$ (0.021 $\text{\AA}/\text{pix}$ in 2x2 binning) for the 2nd order of VS and 0.0066 $\text{\AA}/\text{pix}$ (0.013 $\text{\AA}/\text{pix}$ in 2x2 binning) for the 2nd order of HS around 4000 \AA , respectively, when we use the above-mentioned demagnification lens unit. The width of the slit is

selectable from 10 μ m (0.0640"), 20 μ m (0.128"), 50 μ m (0.320"), 100 μ m (0.640"), and 200 μ m (1.28").

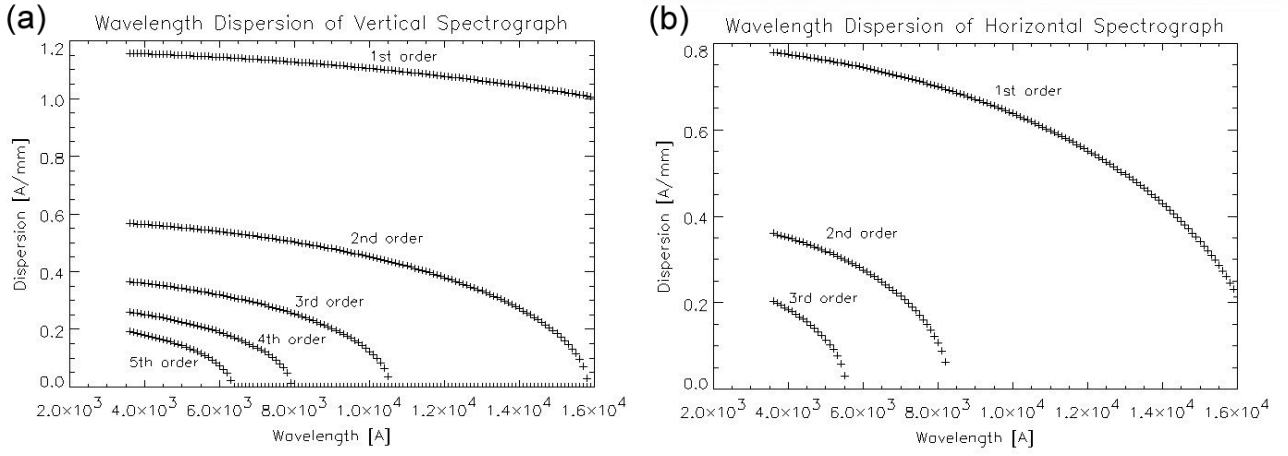


Fig. 2 Wavelength dispersion of Vertical Spectrograph (a) and Horizontal Spectrograph (b).

The exposure time depends on the observing wavelength, order of the spectrum, slit width and the sky condition. In typical Ca II K, H observations with HS, in which we use slit width of 100 μ m (0.640"), the appropriate exposure is usually 50 – 100 msec. Thus scanning speed of about 6.40 – 12.8 arcsec/sec can be attained with the spatial step of 0.640 arcsec.

Image scan is performed by tilting a glass block placed in front of the slit of the spectrograph. The glass block is made of BK7 and has optical quality surfaces with a thickness of 50mm. It is mounted on a high precision rotating stage driven by a stepping motor, so that the solar image on the slit can be translated in a direction perpendicular to the slit with a spatial resolution of 0.0049 arcsec. The speed of image motion can be set with the observation control software in a range of 0.0049 - 49 arcsec/sec depending on optimized exposure time and desired spatial resolution. Maximum range of scan is approximately ± 200 arcsec. Note that spectroheliograph observations in 2007, some of which are described in papers of this special issue, were performed by moving the telescope, since this scanning device was installed in 2008.

At present, we have two Prosilica CCD cameras, with which we can observe two spectral regions simultaneously on the horizontal spectrograph. Each CCD camera is controlled by a Windows PC via the ethernet interface. Data are transferred through the same line and stored in a local hard disk. Partial area on the CCD can be selected for actual data transfer to save the data size and storage time. Another PC that controls the observation sequence operates the rotation stage to tilt the glass block via a serial interface, and sends triggering signals to start and stop the data collection to other PC's that operate the CCD's through a digital I/O interface.

Reflected light at the slit mirror is fed to a slit jaw imaging system by a $\times 0.5$ demagnification relay lens. In this path we have a tunable $H\alpha$ Lyot filter with a passband of $0.25/0.50 \text{ \AA}$. A 2048×2048 pixel CCD camera with a mechanical shutter (Kodak Megapixels 4.2i) takes the $H\alpha$ images in a plate scale of $0.138 \text{ arcsec/pixel}$. A PC is dedicated to operate the CCD camera and the wavelength of the Lyot filter; in usual observations, we take $H\alpha$ images at the center, $\pm 0.5 \text{ \AA}$, and $\pm 0.8 \text{ \AA}$ sequentially in parallel with the spectrographic observations. In figure 3, we show photographs in which arrangement of optical elements and devices for the two spectrographs can be seen.

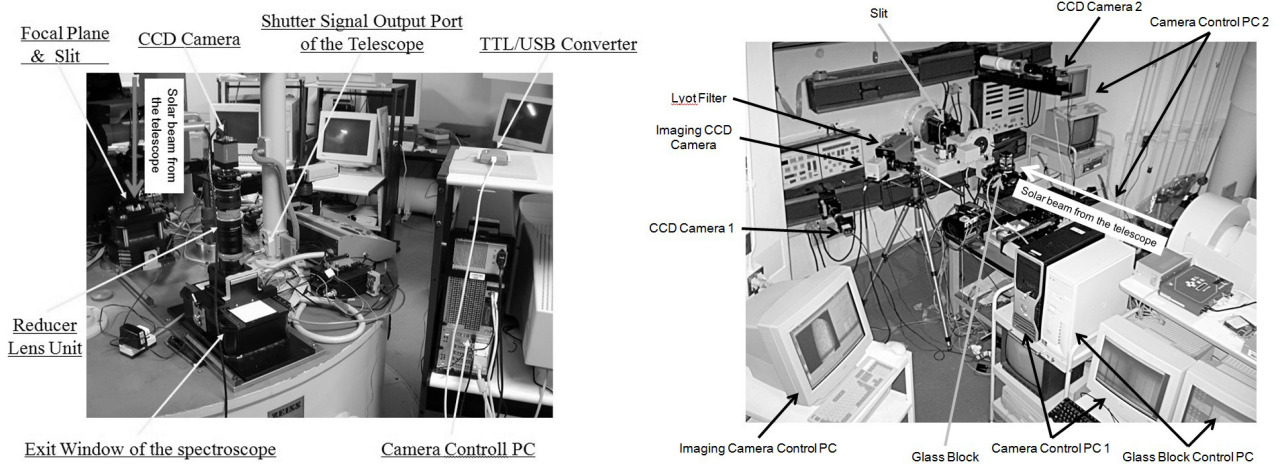


Fig. 3 Photograph in VS room (left picture) and HS room (right picture).

The procedure to obtain a flat field for the spectral images is shown in figure 4. In this procedure, we average a number of quiet sun spectra after the dark-reduction, and moreover create an artificial spectrum image by averaging it in spatial and spectral directions. From the distribution of the ratio between these two kinds of averaged frames, we can obtain an artificial flat field. Finally, we can make calibrated spectrum image by dividing a raw spectrum image by the artificial flat field after the dark-reduction.

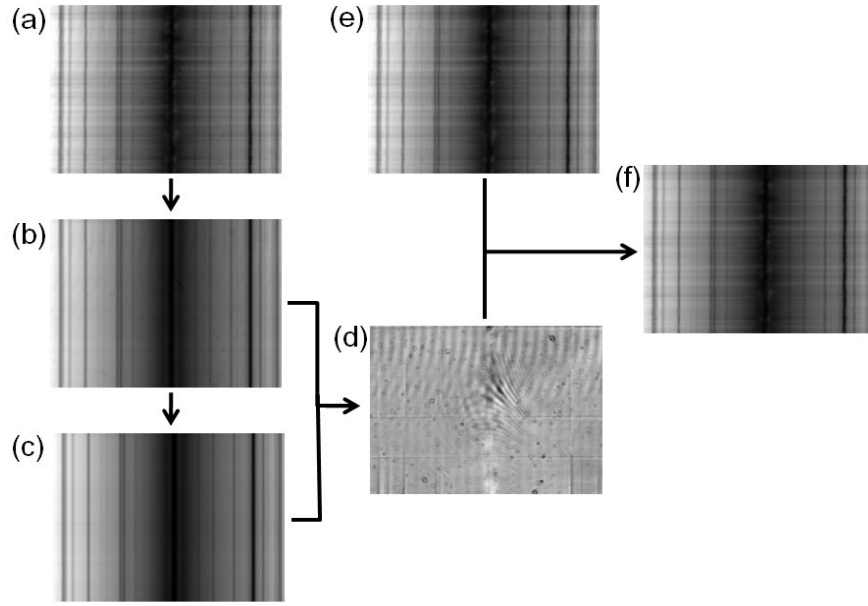


Fig. 4 The process of flat-field calibration. (a) a quiet region spectrum. (b) an averaged frame of 1000 quiet region spectra: $B(x,y)$. (c) an artificial averaged frame: $C(x,y) = (\int B(x,y)dy) \otimes (\int B(x,y)dx)$. (d) the artificial flat field: $D(x,y) = B(x,y)/C(x,y)$. (e) each data frame of the spectrum: $E(x,y)$. (f) the calibrated frame: $F(x,y) = E(x,y)/D(x,y)$.

4. Example of observation

Figure 5 shows an example of CaII K spectroheligram around the solar limb which was taken on 5th August 2007 with the VS in 2nd order. The slit width is 100 μm , exposure time for each frame at a slit position is 0.090 s and 2x2 summing on CCD. On the solar disk, we can find three dimensional

structures of the chromosphere through the different wavelength heliograms. On the other hand, out of the limb, the differences of the Doppler velocity field in the prominence and spicules are obvious.

Figure 6 also shows an example of CaII K spectroheliogram around a sunspot region which was taken on 7th August 2007 with the VS in 2nd order. The slit width and CCD binning size are the same as figure 5, but exposure time for each frame at a slit position is 0.070 s. In this case, the scan width is 120 arcsec and the time for one scan is about 12 sec. In this figure, we can clearly see emerging fluxes at the right-side of the sunspot and a number of fibril structures between bright boundaries of supergranulations, especially in the upper chromosphere.

An example of simultaneous multi-wavelength observation is shown in figure 7. Though both Ca II K line and H α line are formed in the solar chromosphere, the intensity patterns of each heliogram are significantly different. This implies that the intensities in the two lines are sensitive to different physical quantities in the chromospheres and suggests a potential capability for better diagnosis for physical conditions in the chromospheres.

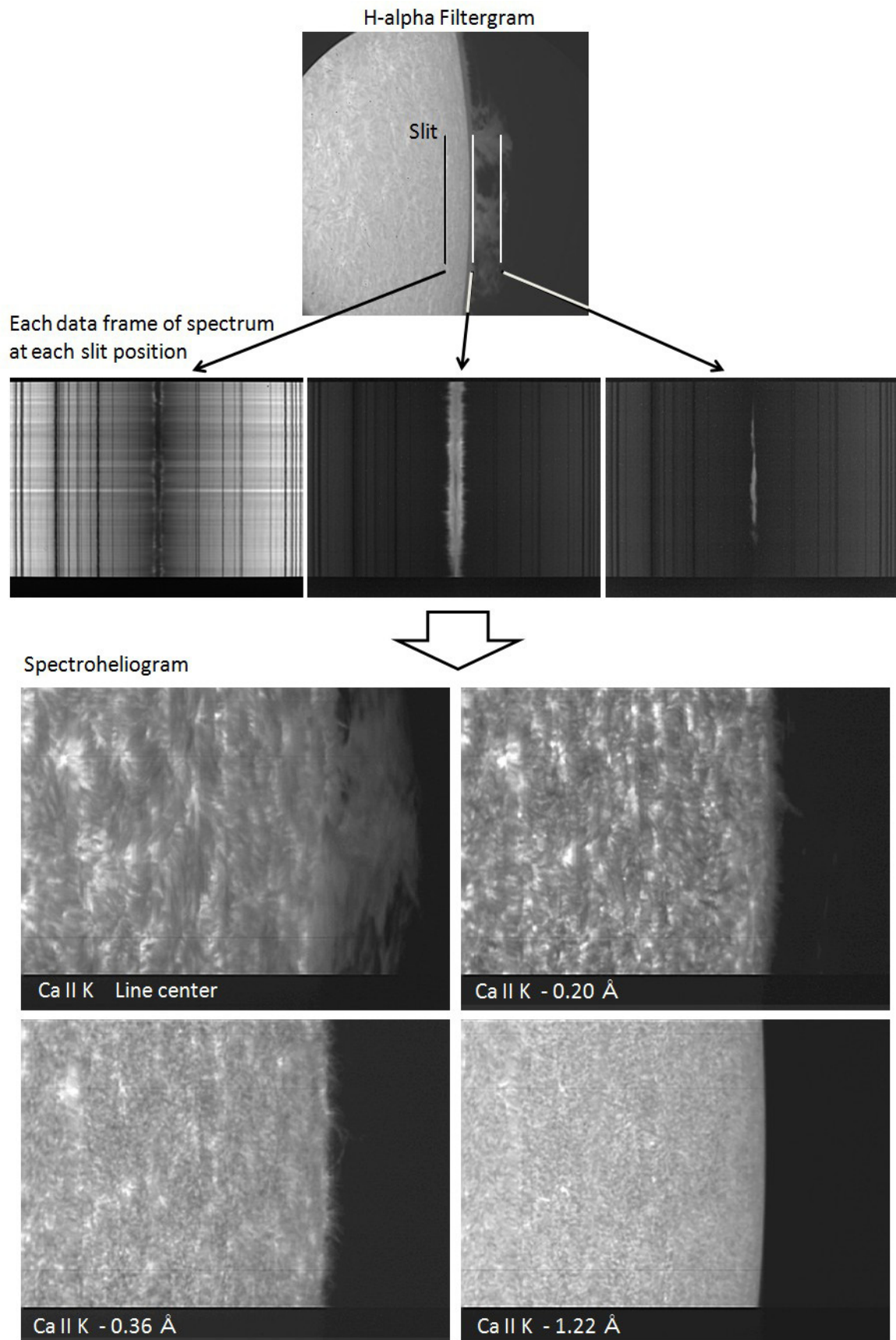


Fig. 5 An example of spectroheliogram around the solar limb with VS.

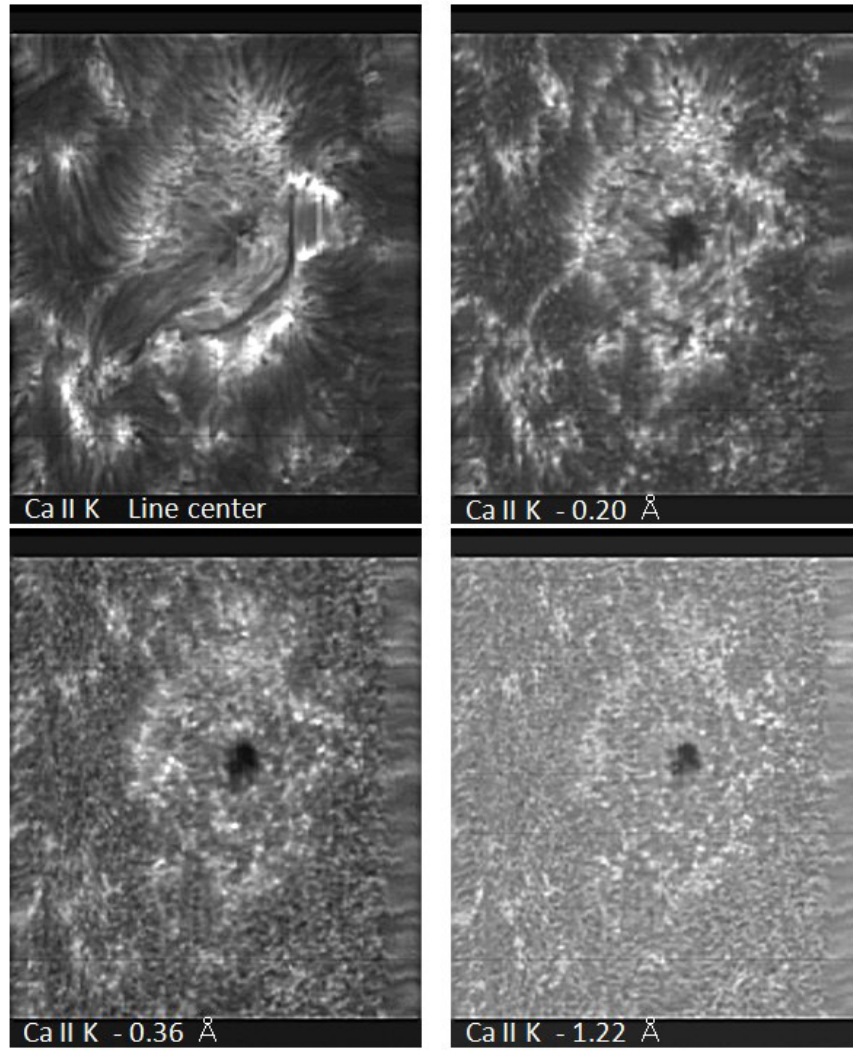


Fig. 6 An example of spectroheliogram around a sunspot region with VS.

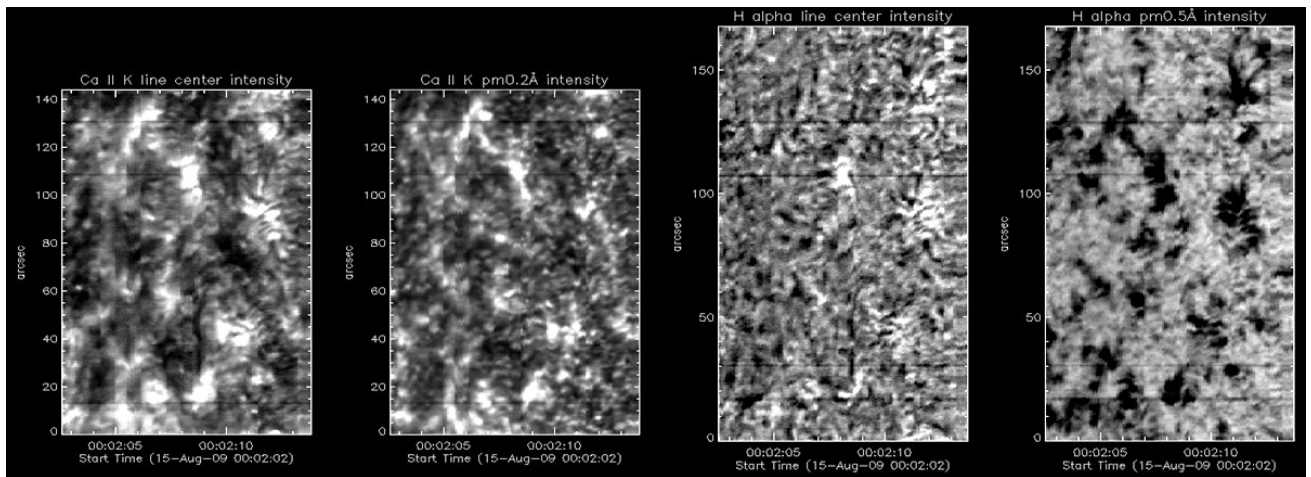


Fig. 7 An example of multi-wavelength observation with HS. From the left, spectroheliograms around the quiet sun in Ca II K line center, Ca II K ± 0.20 Å, H α line center, H α ± 0.50 Å, obtained on 15th August 2009 at the 1st and 2nd order of HS for Ca II K and H α , respectively.

5. Conclusion

By using high sensitivity, fast readout CCD cameras together with the image scanning mechanism on the DST at Hida observatory, the new observing system enable us high cadence, high resolution and high accuracy spectroheliograph observations of the sun at any wavelength from visible to near IR. Especially, with multiple cameras on horizontal spectrograph, we can make simultaneous observations at different wavelengths with a flexible choice of lines. The system is complementary with the filter-based 2D spectrograph systems such as IBIS at NSO (Cavallini 2006) or CRISP at SST (Scharmer et al. 2008) in a sense that our system allows to get more spectral information including different spectral lines but with a less applicability of image reconstruction technique. The system is also highly complementary with the SOT aboard Hinode, and coordinated observations with Hinode are expected to open the new era of the solar chromospheric study.

Acknowledgements

This work was supported by the Grant-in-Aid for the Global COE Program "The Next Generation of Physics, Spun from Universality and Emergence" from the Ministry of Education, Culture, Sports, Science and Technology (MEXT) of Japan.

This work was also supported by the Grant-in-Aid for Creative Scientific Research "The Basic Study of Space Weather Prediction" (17GS0208, Head Investigator: K. Shibata) from the MEXT of Japan.

Moreover, we thank the following people's supports in the fields of data acquisitions, campaign observations, and automation of this system: Messrs. N. Kaneda, K. Otsuji, Y. Hashimoto, T. Anan, H. Watanabe, T. Kawate and Drs. T.T. Ishii, K. Nishida, T. Matsumoto, Y. Hanaoka, S. Kamio, H. Isobe, A. Asai.

References

Cavallini F., 2006, Solar Physics, 236, 415

De Pontieu B., McIntosh S.W., Carlsson M., Hansteen V.H., Tarbell T.D., Schrijver C.J., Title A.M., Shine R.A., Tsuneta S., Katsukawa Y., Ichimoto K., Suematsu Y., Shimizu T., Nagata S., 2007, Science, 318, 1574

Hanaoka Y., 2003, SPIE, 4853, 584

Ishikawa R., Tsuneta S., Ichimoto K., Isobe H., Katsukawa Y., Lites B.W., Nagata S., Shimizu T., Shine R.A., Suematsu Y., Tarbell T.D., Title A.M., 2008, A&A, 481, L25

Katsukawa Y., Berger T.E., Ichimoto K., Lites B.W., Nagata S., Shimizu T., Shine R.A., Suematsu Y., Tarbell T.D., Title A.M., Tsuneta S., 2007, Science, 318, 1594

Lites B.W., Socas-Navarro H., Kubo M., Berger T., Frank Z., Shine R.A., Tarbell T.D., Title A.M., Ichimoto K., Katsukawa Y., Tsuneta S., Suematsu Y., Shimizu T., 2007, Publications of the Astronomical Society of Japan, 59, S571

Nakai Y., Hattori A., 1985, Kyoto Univ. Faculty of Sci Memoirs Series of Physics, Astrophysics, Geophysics and Chemistry, 36, 385

Ning Z., Cao W., Okamoto T.J., Ichimoto K., Qu Z.Q., 2009, A&A, 499, 595

Okamoto T.J., Tsuneta S., Berger T.E., Ichimoto K., Katsukawa Y., Lites B.W., Nagata S., Shibata K.,

Shimizu T., Shine R.A., Suematsu Y., Tarbell T.D., Title A.M., 2009, Science, 318, 1577

Scharmer G.B., Narayan G., Hillberg T., de la Cruz Rodriguez J., Lofdahl M.G., Kiselman D., Sutterlin P., van Noort M., Lagg A., 2008, ApJ, 689, L69

Shibata K., Nakamura T., Matsumoto T., Otsuji K., Okamoto T.J., Nishizuka N., Kawate T., Watanabe H., Nagata S., UeNo S., Kitai R., Nozawa S., Tsuneta S., Suematsu Y., Ichimoto K., Shimizu T., Katsukawa Y., Tarbell T.D., Berger T.E., Lites B.W., Shine R.A., Title A.M., 2007, Science, 318, 1591